Carbohydrate Polymers 89 (2012) 403–410

Contents lists available at SciVerse ScienceDirect

Carbohydrate Polymers

journal homepage: www.elsevier.com/locate/carbpol

N-hexanoyl, N-octanoyl and N-decanoyl chitosans: Binding affinity, cell uptake, and transfection

Buddhadev Layek, Jagdish Singh*

Department of Pharmaceutical Sciences, College of Pharmacy, Nursing, and Allied Sciences, North Dakota State University, Fargo, ND 58105, USA

ARTICLE INFO

Article history:
Received 6 December 2011
Received in revised form 5 March 2012
Accepted 7 March 2012
Available online 16 March 2012

Keywords:
Chitosan
Short chain fatty acid
Cell uptake
Transfection efficiency
Gene delivery

ABSTRACT

Low transfection efficiency of chitosan limits its use as a non-viral vector for practical purposes. This study was designed to investigate the effect of fatty acyl chain length on physicochemical properties, pDNA binding affinity, cell uptake, and in vitro transfection efficiency of N-acyl chitosan (NAC). NAC polymers were synthesized by carbodiimide mediated coupling reaction of chitosan with n-hexanoic, n-octanoic, and n-decanoic acid, respectively. These NAC polymers effectively condensed pDNA resulting in the size range of 220–342 nm with net positive charge. NAC polymers also showed good pDNA binding capacity, high protection of pDNA from nuclease degradation and excellent biocompatibility. Transfection efficiency of chitosan, in HEK 293 cells, was enhanced 15–25-fold after coupling with fatty acid and increased with a decrease in fatty acyl chain length of NAC. Thus, the present study demonstrates that the NAC polymers hold great potential as novel non-viral gene delivery vector.

1. Introduction

Chitosan [β (1 → 4) linked 2-amino-2-deoxy-β-D-glucan] is a linear copolymer of N-acetyl-D-glucosamine and D-glucosamine produced by alkaline deacetylation of chitin. Chitosan and its derivatives have been extensively used in various biomedical applications (Hirano, Kaneko, & Kitagawa, 1991; Jayakumar et al., 2010; Muzzarelli, 1983; Muzzarelli, Frega, Miliani, Muzzarelli, & Cartolari, 2000) due to their biodegradability, excellent safety profile, low immunogenicity, favorable physicochemical properties, and ease of chemical modification (Lee, Kwon, Kim, Jo, & Jeong, 1998; Li et al., 2010; Zhu, Pan, Liao, Zhao, & Chen, 2008). At low pH (below the pK_a of 6.5), primary amines of the chitosan backbone remain positively charged and can form complexes with negatively charged DNA through ionic interactions, thereby condensing it into small particles and protecting it from DNase-I & II degradation (Chang, Higuchi, Kawakami, Yamashita, & Hashida, 2010; Huang, Fong, Khorc, & Lim, 2005; Koping-Hoggard et al., 2001). However, the main drawback of chitosan-based delivery systems is their low transfection efficiency at physiological conditions. The low transfection efficiency of chitosan-based delivery systems is primarily attributed to the poor water solubility at physiological pH (Chen, Ding, Qu, & Zhang, 2008) and the inability to release DNA after endosomal escape due to strong interaction between chitosan and DNA (Lu et al., 2009). Several modifications of chitosan side chains using hydrophilic (Germershaus, Mao, Sitterberg, Bakowsky, & Kissel, 2008; Park et al., 2000), hydrophobic (Hu et al., 2006; Jayakumar et al., 2010; Liu et al., 2003; Sajomsang, Ruktanonchai, Gonil, Mayen, & Opanasopit, 2009), and both hydrophilic–hydrophobic moieties (Wang, He, Tang, & Yin, 2011) have been reported to enhance the transfection efficiency of chitosan. Modification with hydrophilic units improves the water solubility and increases the plasma circulation time of the polyplexes. Hydrophobic modification of chitosan alters polyplex interaction with the cell membrane, facilitates intracellular DNA dissociation, and improves water solubility (Kim et al., 2007).

The expression of transferred gene occurs only after the DNA is transported into the nucleus of a target cell. Therefore, the vectors for gene delivery must be able to overcome a number of extracellular and intracellular barriers. These include various endonucleases present in the extracellular space that can degrade the plasmid DNA within 30 min (Kawabata, Takakura, & Hashida, 1995). Another major barrier is the inability of the plasmid DNA to cross the biological membrane due to the repulsion between the DNA and the negatively charged cell surface. Even after crossing the cell membrane, the DNA has to escape lysosomal degradation and translocate into the nucleus (Wiethoff & Middaugh, 2003). Hence, the balance between DNA protection and intracellular DNA release significantly influence transfection efficiency of chitosan-based gene delivery systems by modulating the degree of interaction between polymeric vectors and their DNA cargo (Chen, Ho, et al., 2008; Koping-Hoggard et al., 2004). However, there are no

* Corresponding author. Tel.: +1 701 231 7943; fax: +1 701 231 8333.
E-mail address: Jagdish.Singh@ndsu.edu (J. Singh).

0144-8617/$ – see front matter © 2012 Elsevier Ltd. All rights reserved.
doi:10.1016/j.carbpol.2012.03.021

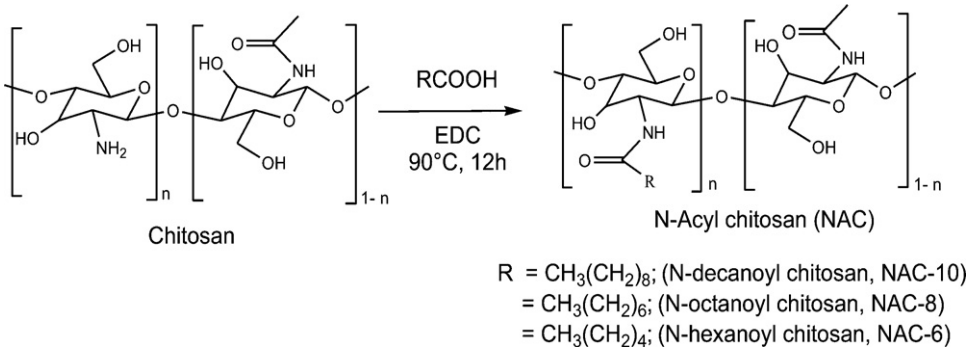

Fig. 1. Synthetic route for N-acyl chitosan (NAC) polymers.

systematic studies on hydrophobic modification of chitosan to describe the optimum balance between polyplex stability and intracellular unpacking of DNA.

In the present report, a series of fatty acids with increasing chain length (C6–C10) were utilized to synthesize N-acyl chitosan polymers. The influence of fatty acid chain length was investigated by assessing the water solubility, particle size, zeta potential, pDNA binding affinity, pDNA release, cellular uptake, in vitro biocompatibility and transfection efficiencies.

2. Experimental

2.1. Materials

Chitosan (Mw ~ 50 kDa, 91% deacetylated) and 3-(4,5-dimethylthiazol-2-yl)-2,5-diphenyl-tetrazolium bromide (MTT) were purchased from Sigma–Aldrich (St. Louis, MO, USA). Capric, caprylic, and caproic acid were procured from MP Biomedicals (Solon, OH, USA). 1-Ethyl-3-(3-dimethylaminopropyl) carbodiimide hydrochloride (EDC.HCl) was obtained from Creosalus Inc. (Louisville, KY, USA). DNase-I was purchased from Rockland Inc. (Gilbertsville, PA, USA). Hoechst 33342 dye was purchased from Anaspec (Fremont, CA, USA). Plasmid DNA encoding green fluorescence protein (gWiz-GFP) and beta-galactosidase (gWiz-βGal) were purchased from Aldevron LLC (Fargo, ND, USA). Human embryonic kidney (HEK 293) cell line, Eagle's minimal essential medium (EMEM), and phosphate buffered saline (PBS) were purchased from American Type Culture Collection (ATCC, Rockville, MD, USA). FuGENE® HD was obtained from Roche Diagnostics (Indianapolis, IN, USA). Beta-galactosidase enzyme assay kit with reporter lysis buffer and agarose were supplied by Promega (Madison, WI, USA). All other reagents were analytical grade and used without further modification.

2.2. Synthesis and characterization of fatty acid coupled chitosan

NAC polymers were synthesized by coupling the carboxyl group of fatty acids with amine group of chitosan in the presence of EDC (Hu et al., 2006) (Fig. 1). Briefly, chitosan (1 g) was dissolved in 100 mL distilled water. Fatty acids (the charged fatty acid ratio was 20% of D-glucosamine units in chitosan) and EDC (5 mol/mol of fatty acid) were dissolved in ethanol. The chitosan solution was heated to 90 °C and the fatty acid solution containing EDC was added drop wise to the chitosan solution under vigorous stirring. The reaction was continued at 90 °C for 12 h. After that, the reaction mixture was dialyzed using SnakeSkin^R Pleated Dialysis tubing (MWCO: 3.5 kDa, Thermo Scientific, IL, USA) against distilled water for 48 h with successive exchange of distilled water to remove the water-soluble by-products. The dialyzed suspension was then dried in a freeze dryer and washed several times with ethanol to remove the unreacted fatty acid. Finally, the precipitate was lyophilized to get the NAC polymers. The overall yield of the reaction was 88, 85 and 83% for decanoic (NAC-10), octanoic (NAC-8), and hexanoic acid (NAC-6) derivative of chitosan, respectively.

The coupling of fatty acid on chitosan backbone was confirmed by proton nuclear magnetic resonance (^{1}H NMR) and Fourier transform-infrared (FTIR) spectroscopy. For ^{1}H NMR experiments, chitosan and NAC polymers were dissolved in D_2O with 1% DCl and D_2O, respectively. ^{1}H NMR spectra were measured using a Mercury Varian 400 MHz spectrometer at 25 °C. FTIR analyses were made using a Thermo Nicolet Nexus 470 FT-IR spectrometer equipped with a N_2 purged chamber. All samples were ground with KBr powder and compressed to form pellets for the study. The degree of substitution of the polymers was determined from the elemental analysis data.

The water solubility of chitosan and NAC polymers was assayed by the turbidity measurements method as a function of pH (Toh, Chen, Lo, Huang, & Wang, 2011). Briefly, chitosan or NAC polymers were dissolved in 0.25% (v/v) acetic acid solution (2 mg/mL). The pH of the solution was adjusted by the addition of 1 N NaOH solution, and then transmittance of the solution was measured at 600 nm using a SpectraMax M5 microplate reader (Molecular Devices, CA, USA).

The buffer capacity of chitosan and synthesized polymers was determined by acid–base titration assay (Benns, Mahato, & Kim, 2002). Briefly, 20 mg of each sample was dissolved in 20 mL of 150 mM NaCl solution. The pH of each solution was adjusted to 10 by the addition of 0.1 N NaOH solutions. The titration was performed by stepwise addition of 20 μL of 0.1 N HCl followed by pH measurements at 25 °C using a pH meter.

2.3. Polyplex formation and characterization

Chitosan and NAC polymers were dissolved into 20 mM sodium acetate buffer with different concentration at pH 6.5. The polymer/pDNA polyplexes of various N/P ratios (the N/P ratio was calculated from the number of unreacted free primary amino groups of polymer and the number of phosphate groups of pDNA) were prepared by drop wise addition of appropriate volume of polymeric solution into the pDNA solution (0.2 mg/mL in 20 mM sodium acetate buffer), while vortexing at high speed for 30 s. The mixture was incubated at room temperature for 30 min to achieve a stable polyplex. The average hydrodynamic diameter and zeta potential of the polyplexes were determined by dynamic light scattering method using a Zetasizer Nano ZS 90 (Malvern Instruments, Malvern, UK) at 25 °C. The size and zeta potential of each polyplex were measured six times. The morphology of the polyplexes was observed by DI-3100 AFM instrument (Veeco, MN, USA) using the tapping mode. For AFM study polyplexes were diluted with

distilled water and a small drop of the samples was placed onto a freshly cleaved mica plate, followed by air drying.

Association efficiency of pDNA was determined by centrifuging NAC/pDNA polyplexes at 30,000 × *g*, at 4 °C for 30 min. The amount of unbound pDNA in the supernatant was measured with a SpectraMax M5 microplate reader using Hoechst dye 33342. The excitation and emission wavelengths were fixed at 350 and 450 nm, respectively. The association efficiency of different polyplexes was calculated by the following equation.

$$\text{association efficiency} = \frac{\text{DNA}_{\text{total}} - \text{DNA}_{\text{free}}}{\text{DNA}_{\text{total}}} \times 100\%$$

2.4. Agarose gel retardation assay

The pDNA condensing capability of the polyplexes was further examined by agarose gel retardation assay at different N/P ratios. Polymer/pDNA polyplexes (containing 1 μg of pDNA) at different N/P ratios were electrophoresed on 0.8% (w/v) agarose gel containing 0.5 μg/mL ethidium bromide (EB) at 80 V for 80 min. The 0.5× Tris-acetate-EDTA (TAE, Bio-Rad, CA, USA) buffer was used as a running buffer. DNA bands were visualized and photographed by the Fluorchem 5500 imager (Alpha Innotech, CA, USA).

2.5. Isothermal titration calorimetry analysis

Isothermal titration calorimetry (ITC) was employed to determine the binding constant, enthalpy of complex formation and the stoichiometry of binding of pDNA with chitosan based cationic polymers. Binding studies were performed using a low volume nano ITC (TA instruments, USA) with a cell volume of 190 μL at 25 °C. Samples were degassed for 10 min prior to use. The sample cell was filled with the pDNA solution (50 μg/mL ~0.1515 mM phosphate or nucleotide units) and the reference cell with buffer solution only. The polymeric solution (150 μg/mL ~0.7688 mM of free amino group) was introduced into the thermostated cell by means of a syringe which also stirred at 250 rpm. Each titration consisted of 25 subsequent 2 μL injections each of which were 20 s in duration and were programmed to occur at 400 s intervals.

2.6. Protection of pDNA against nucleases

The ability of polyplexes to protect pDNA from nuclease degradation was examined by DNase protection assay. Naked pDNA or NAC/pDNA polyplexes (20 μL equivalent to 2 μg of pDNA) were incubated with 1 unit of DNase for 30 min at 37 °C. The DNase reaction was stopped by 5 μL of 100 mM EDTA solution. Twenty microliters of heparin (5 mg/mL) was added and incubated for 2 h at room temperature to dissociate the complex. The integrity of released pDNA was evaluated by agarose gel electrophoresis as described under Section 2.4.

2.7. Ethidium bromide exclusion assay

Different amount of chitosan or NAC polymers were complexed with 2 μg (20 μL of 0.1 mg/mL solution) of pDNA to obtain polyplexes of desired N/P ratios and incubated at room temperature for 30 min. The final volume of the polyplexes was adjusted to 1 mL with PBS (pH 7.4). Subsequently 0.5 μg ethidium bromide (10 μL of 0.05 mg/mL) was added and staining was completed at room temperature for 5 min. Fluorescence intensity was measured with SpectraMax M5 plate reader with the excitation wavelength at 260 nm and emission wavelength at 600 nm. Results were represented as relative fluorescence intensity where 0 suggested the existence of EB only and 100% represented the fluorescence of EB combined with pDNA.

2.8. In vitro release of pDNA

A volume of 3 mL of polyplexes (containing 100 μg of pDNA) was dispersed in 30 mL of phosphate buffered saline (PBS, pH 7.4) and incubated at 37 °C in a shaking incubator at 100 rpm. After 0, 1, 2, 4, 6, 10, 20, 30 and 48 h of incubation, 1 mL of sample was withdrawn and replaced with an equal volume of fresh buffer. The complex suspension was centrifuged at 30,000 × *g*, at 4 °C for 30 min, and the amount of free pDNA in the supernatant was quantified by spectrofluorimetry using Hoechst dye 33342. The percent of cumulative release of pDNA was calculated.

2.9. In vitro cytotoxicity

The cytotoxicity of polymers as well as NAC/pDNA polyplexes was evaluated by MTT assay (Lu et al., 2009). HEK 293 cells were seeded in a 96-well plate at a density of 5000 per well in 150 μL of EMEM supplemented with 10% of fetal bovine serum (FBS), and incubated at 37 °C under 5% CO_2 atmosphere. The cytotoxicity of polymers was examined by determining the viability after 48 h of incubation with various concentrations of polymers (100–2000 μg/mL). Similarly, the cytotoxicity of polyplexes was evaluated at various N/P ratios (5, 10, and 20). Non-treated cells were considered as control and incubated in similar conditions for same period of time.

$$\%\,\text{cell viability} = \frac{\text{OD}_{\text{sample}}}{\text{OD}_{\text{control}}} \times 100\%$$

2.10. Cellular uptake of polyplexes

To perform the cellular uptake study the pDNA was covalently labeled with FITC, and was allowed to form polyplexes with chitosan and NAC polymers. HEK 293 cells were seeded at a density of 5×10^4 cells per well in a 48-well plate in EMEM medium containing 10% FBS and incubated for 24 h to achieve ~60–70% confluency. Polyplexes containing 1 μg of pDNA were added to each well and incubated at 37 °C for 4 h. The uptake process was terminated by removing the media containing pDNA/polymer polyplexes and washed with PBS. The percentages of FITC positive cells were determined by fluorescence activated cell sorting (FACS) analysis of the cells using a flowcytometer (Accuri Cytometer Inc., MI, USA).

2.11. Gene transfection efficiency

Transfection assay was performed in HEK 293 cells using two different plasmids encoding for green fluorescence protein (pGFP) and β-galactosidase (pβ-Gal) to evaluate gene transfection efficiency at the cellular and protein level, respectively. Cells were seeded at a density of 5×10^4 cells per well in a 48-well plate in EMEM medium containing 10% FBS and incubated for 24 h to achieve ~60–70% confluency. The culture medium was replaced with 300 μL of FBS free or 10% FBS containing EMEM medium before transfection. Polyplexes containing 1 μg of pDNA were added to each well and incubated at 37 °C. After 6 h of incubation transfecting medium was replaced with 300 μL of complete growth medium and further incubated for 48 h. Non-treated cells and cells transfected with naked pDNA were used as negative control and passive control, respectively. Transfection using FuGENE® HD was used as positive control and was carried out according to the manufacturer's protocol with FBS free or 10% FBS containing medium. The percentages of GFP positive cells were determined by FACS analysis of the transfected cells using a flowcytometer. The images of GFP

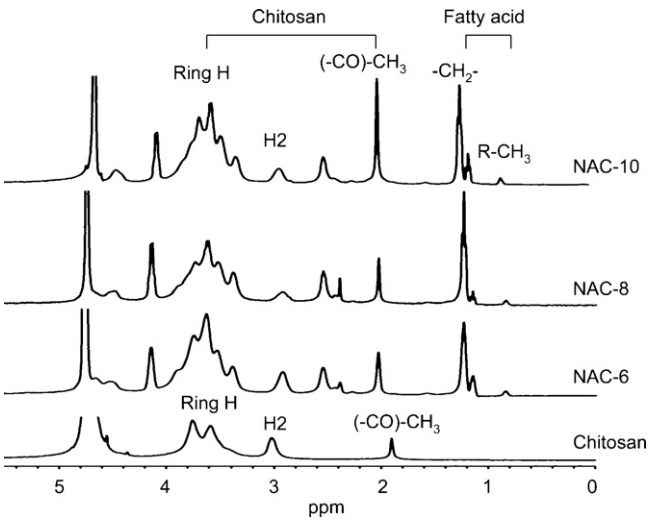

Fig. 2. ^{1}H NMR spectra of chitosan and NAC polymers in D_2O at 25 °C.

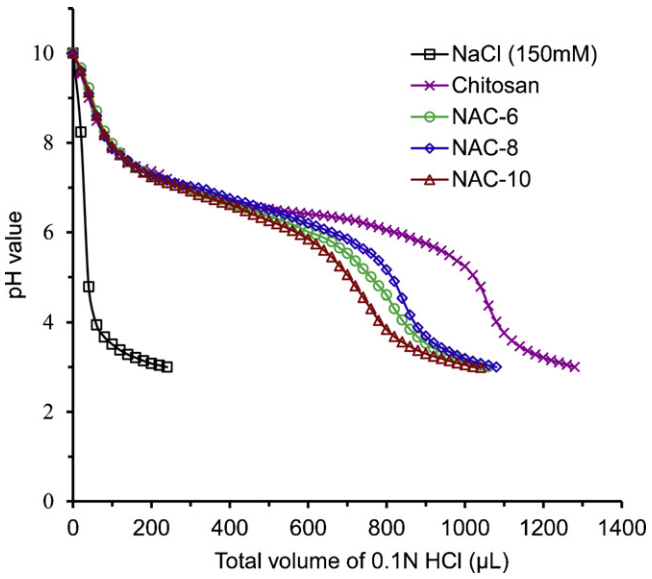

Fig. 3. Buffer capacity of chitosan and different NAC polymers.

transfected cells were taken with a FV300 confocal laser scanning microscope (Olympus, NY, USA). All transfection experiments were performed as replicates of four.

For the β-galactosidase expression, cells were washed twice with PBS (pH 7.4), and lysed using reporter lysis buffer. The β-galactosidase activity was quantified using β-galactosidase assay reagent. The total protein content of the cell lysate was analyzed using a BCA assay kit. The β-galactosidase activity was expressed as milliunit of β-galactosidase/mg of the total protein.

2.12. Statistical analysis

Data are expressed as means ± standard deviation (S.D.). Statistical analyses were performed using two tailed Student's *t*-test and analysis of variance (ANOVA).

3. Results and discussion

3.1. Synthesis and characterization of fatty acid coupled chitosan

The chitosan of 50 kDa molecular weight was chosen based on our preliminary studies with a series of chitosan with different molecular weight ranging from 5 to 100 kDa (maximum transfection was observed with 50 kDa chitosan, data is not shown). The coupling between chitosan and fatty acid was performed by EDC mediated reaction. The excess EDC and water soluble by-products were removed by dialysis with water, and the remaining fatty acid was removed by ethanol washing. The coupling of fatty acid on chitosan backbone was confirmed by ^{1}H NMR and FTIR spectroscopy. The ^{1}H NMR spectra of chitosan and NAC polymers are depicted in Fig. 2. For chitosan, peak at 1.9 ppm revealed the three N-acetyl protons of N-acetyl glucosamine and peak at 3 ppm showed the H_2 proton of N-acetyl glucosamine or glucosamine residue. The ring protons (H-3, 4, 5, 6, 6′) of chitosan are considered to resonate at 3.4–3.8 ppm. The new proton peaks at 0.8 and 1.25 ppm were assigned to $-CH_3$ and $-CH_2$ of the fatty acyl residue, respectively. FTIR spectra were also employed to confirm the coupling of fatty acid on chitosan by observing amide bond formation (Figure S1). The very weak peak at 1655 cm^{-1} for chitosan represented the carbonyl stretching of secondary amide (amide I band). The peak at 1570 cm^{-1} was ascribed to the N—H bending vibration of nonacylated α-aminoglucose primary amines (Tien, Lacroix, Szabo, & Mateescu, 2003). After N-acyl formation, the peak at 1570 cm^{-1} almost disappeared, while very prominent peaks at 1655 and 1555 cm^{-1} were observed. The peak at 1555 cm^{-1} can be assigned to the N—H bending vibrations of the amide II band (Tien et al., 2003). The absorption peaks at 2850–2950 cm^{-1} were due to the $-CH_2$ groups, and their intensity was proportional to the acyl chain length. Hence, the FTIR results confirmed the successful synthesis of NAC polymers. The degree of fatty acid substitution was ~10% for all the three polymers.

The water solubility of chitosan and NAC polymers was studied by measuring the transmittance at 600 nm. The cloud point pH of the polymers has been defined by Mao et al. (2004) as the pH at which the transmittance *T* was higher than 98% at 600 nm. The cloud point pH values of chitosan, NAC-6, NAC-8, and NAC-10 were 6.5, 7.54, 7.52, and 7.54, respectively. Thus, all of the NAC polymers exhibited improved water solubility at neutral pH when compared to the parent chitosan. The improved water solubility of NAC polymers is due to the disruption of H-bonded complex crystal structure of parent chitosan by coupling the short chain hydrophobic moiety to the chitosan backbone (Pillai, Paul, & Sharma, 2009).

The buffer capacity of NAC polymers was determined by acid–base titration assay as described by Lu et al. (2009). According to the proton sponge mechanism, polymers having a buffering capacity between pH 5 and 7 are hypothesized to mediate facilitated endo-lysosomal escape of their cargo due to rupture of the endocytic vesicle caused by an increased osmotic pressure (Godbey, Wu, & Mikos, 1999). As shown in Fig. 3, NAC polymers exhibited very good buffer capacity in the range of pH 5–7.

3.2. Characterization of polymer/pDNA polyplexes

The polymer/pDNA poyplexes were prepared in 20 mM sodium acetate buffer at pH 6.5. Due to the positive charge, these polymers effectively condensed pDNA through electrostatic interaction to form nano-scale polyplexes. The average hydrodynamic diameter and zeta potential of polyplexes at different N/P ratios are summarized in Table 1. The average size of the polyplexes was in the range of 220.1–342.1 nm with a polydispersity index of 0.11–0.22. The polyplexes diameters were found to decrease with an increase in N/P ratio from 5 to 20, which was due to better condensation of pDNA by the protonated amine groups of the polymers. The polyplexes maintained a net positive charge at pH 6.5 between N/P ratios of 5–20. The zeta potential of the polyplexes was directly proportional to their N/P ratio. The surface morphology of the

Table 1
Sizes, zeta potentials, and association efficiency of NAC/pDNA polyplexes at pH 6.5. Indicated values were mean ± S.D. ($n = 6$).

Polyplexes	N:P ratio	Particle size (nm)	PDI[a]	Zeta potential (mV)	Association efficiency (%)[b]
NAC-6/pDNA	5	308.9 ± 7.7	0.21 ± 0.02	14.3 ± 0.6	96.5 ± 2.5
	10	248.4 ± 10.6	0.13 ± 0.03	18.2 ± 0.7	
	20	220.1 ± 1.6	0.11 ± 0.04	20.3 ± 0.8	
NAC-8/pDNA	5	339.7 ± 5.0	0.22 ± 0.02	14.8 ± 0.7	97.8 ± 3.5
	10	268.1 ± 7.4	0.13 ± 0.01	16.4 ± 0.9	
	20	244.9 ± 4.4	0.12 ± 0.02	20.4 ± 0.5	
NAC-10/pDNA	5	342.1 ± 13.5	0.22 ± 0.05	13.3 ± 0.6	96.2 ± 3.1
	10	271.1 ± 5.0	0.13 ± 0.03	15.8 ± 0.4	
	20	246.4 ± 5.6	0.11 ± 0.01	19.9 ± 0.9	

[a] Particle dispersity index.
[b] Association efficiency measured at N/P ratio of 20.

polyplexes was visualized by AFM and the polyplexes observed were nearly spherical in shape (Figure S2). The association efficiency of the polyplexes was ~97% at N/P ratio of 20 (Table 1).

3.3. Agarose gel retardation assay

Neutralization of negative charges on the phosphate backbone of pDNA by the positively charged polymeric nano-complexes resulted in the retardation of mobility of pDNA under the influence of an electric field. Fig. 4A shows pDNA binding capacity of polyplexes at different N/P ratios. The movement of naked pDNA towards the anode was observed in Lane a. We observed only a slight retardation of mobility of pDNA at N/P ratio of 0.5 and 1 (Lanes b and c). However, the complete retardation of the pDNA was observed at N/P ratio of ≥5, indicating the tight complexation between polymeric nano-complexes and pDNA.

3.4. ITC

ITC was used to investigate the pDNA binding capacity of chitosan and NAC polymers. The heat change (ΔQ) per injection was represented as a function of the corresponding N/P ratio (Figure S3). The heat of dilution from titrations of polymer solution into buffer only was subtracted to get net binding heat changes. The isotherms were fitted to an independent model using Nanoanalyze software. The thermodynamic parameters such as the pDNA binding constant, enthalpy of complex formation and the stoichiometry of binding of pDNA with chitosan based cationic polymers are presented in Table S1. The binding affinity of NAC polymers ($(21.15–22.90) \times 10^5\ M^{-1}$) was significantly lower than the chitosan ($28.79 \times 10^5\ M^{-1}$), but it did not change significantly among the different NAC polymers with similar degrees of substitution suggesting that the fatty acid chain length had no effect on binding affinity of the polymers.

3.5. Protection of pDNA against nucleases

The integrity of pDNA is essential for efficient gene delivery in vitro as well as in vivo, and therefore the gene delivery system should effectively protect condensed pDNA from nuclease degradation (Katayose & Kataoka, 1998). The protective effect of polyplexes against nuclease degradation was evaluated using DNase-I as a model enzyme (Fig. 4B). It turned out that the naked DNA was completely digested as indicated by the absence of band for DNA. All three NAC polymers exhibited distinct protective activity against DNase-I at all N/P ratios tested. These results clearly indicated that NAC polymers can be used as efficient vector for transporting pDNA into the cytoplasm of cell without degradation.

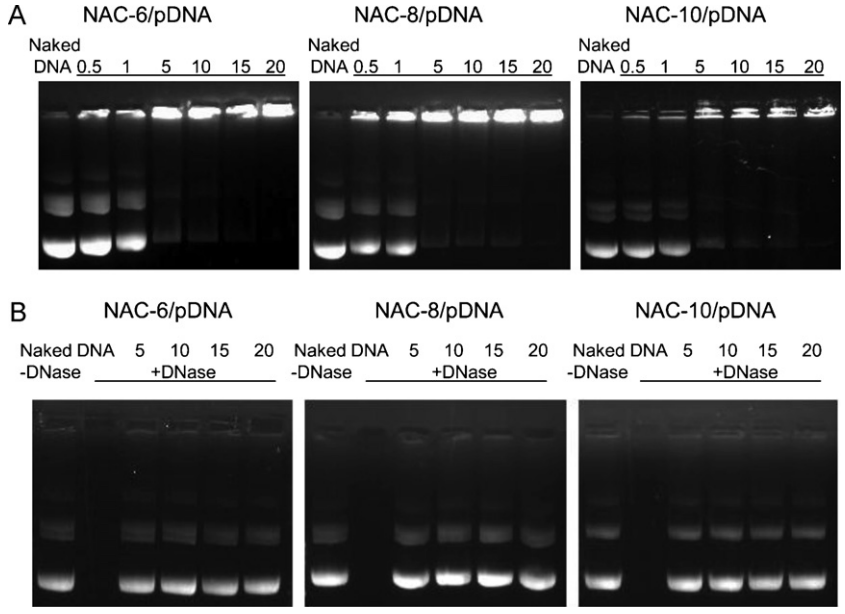

Fig. 4. (A) Agarose gel retardation assay to test pDNA binding capacity of NAC/pDNA polyplexes at different N/P ratios. (B) DNase-I protection assay to evaluate the pDNA protective effect of NAC/pDNA polyplexes against nuclease degradation at different N/P ratios.

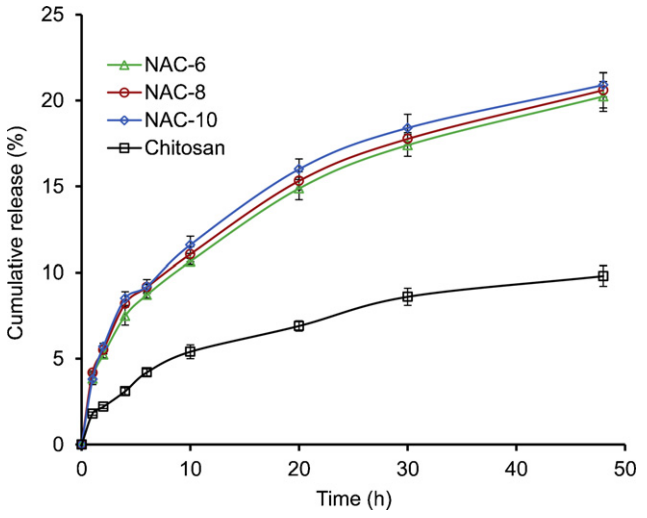

Fig. 5. Cumulative pDNA release profiles of NAC-6/pDNA, NAC-8/pDNA, and NAC-10/pDNA polyplexes at N/P ratio of 20 and chitosan/pDNA polyplexes at N/P ratio of 5 after exposing to PBS (pH 7.4) at 37 °C. Indicated values were mean ± S.D. ($n = 4$).

3.6. Ethidium bromide exclusion assay

The binding affinity between NAC polymers and pDNA was evaluated by EB exclusion in PBS (pH 7.4) to correlate the pH environments in the cytoplasm and nuclei (Wang et al., 2011). It was found that the EB fluorescence intensity decreased with higher N/P ratio (Figure S4). At N/P ratio 20, fluorescence quenching percentages of chitosan/pDNA, NAC-6/pDNA, NAC-8/pDNA and NAC-10/pDNA polyplexes were 90.3%, 80.2%, 79.3% and 78.6%, respectively.

3.7. In vitro release of pDNA

Fig. 5 revealed the in vitro release profile of pDNA from the polyplexes prepared at N/P ratio of 20 for NAC polymers and at N/P ratio of 5 for chitosan. These N/P ratios were selected based on their transfection efficiency. For chitosan maximum transfection efficiency was achieved at N/P ratio of 5 while NAC polymers showed maximum transfection at N/P ratio of 20 (data not shown). The release of pDNA was slow over the period of 48 h. The cumulative release of pDNA prepared with chitosan was less than 10% at 48 h. However, there was a relatively rapid release of pDNA prepared with NAC with the cumulative release of ~20%, but no significant differences ($p > 0.05$) existed among the three different polyplexes. Fatty acid substitutions of chitosan facilitate the pDNA dissociation due the substitution of a fraction of free amino groups as well as hydrophobicity-induced weakening of the electrostatic interaction between the polymer and pDNA (Wang et al., 2011).

3.8. Cell viability

One important criterion of gene delivery vectors is low cytotoxicity. It has been reported that cationic agents may cause severe cytotoxicity due to interactions with cell membrane and other negatively charged cellular components or proteins (Choksakulnimitr, Masuda, Tokuda, Takakura, & Hashida, 1995; Fischer, Li, Ahlemeyer, Krieglstein, & Kissel, 2003). It has been established that chitosan and its derivatives are less cytotoxic than other cationic polymers such as poly-lysine and polyethyleneimine. Nevertheless, their toxicity depends on the type of chitosan derivative as well as the type of cells studied (Fischer et al., 2003; Thanou, Florea, Geldof, Junginger, & Borchard, 2002). In this study we used MTT assay to evaluate the toxicity of different polymers and polymer/pDNA polyplexes in

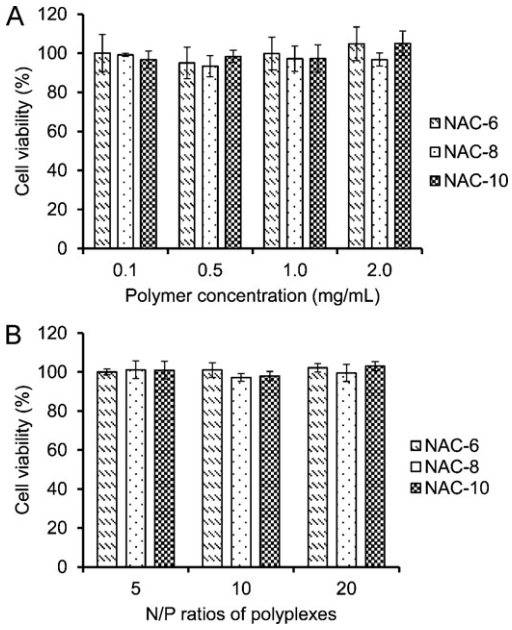

Fig. 6. In vitro cytotoxicity of (A) NAC polymers and (B) NAC/pDNA polyplexes in HEK 293 cells. Data were expressed as mean ± S.D. ($n = 4$).

HEK 293 cells. As depicted in Fig. 6A, NAC polymers did not exhibit significant ($p > 0.05$) change in cell viability at the tested concentrations. Similarly, polyplexes at different N/P ratios did not alter the cell viability (Fig. 6B) in comparison to the control (taken as 100% viability). Therefore, MTT assay results confirmed an excellent in vitro biocompatibility of the polymers as well as polyplexes, which is critical for the development of successful non-viral gene delivery systems.

3.9. Cellular uptake study

For chitosan/pDNA polyplexes only 15% of cells were FITC-positive while cellular uptake of different NAC/pDNA polyplexes was elevated by 5–7-fold. Since NAC polymers consist of both cationic amino groups and hydrophobic fatty acyl moieties, both charge attraction and hydrophobic interactions play an important role in the cellular uptake process by endocytosis (Piest & Engbersen, 2010). NAC-6 polyplex exhibited highest degree of cellular uptake with 90% cells was FITC-positive. The cellular uptake of NAC/pDNA polyplex was increased as the chain length of fatty acid substituent decreased. The uptake percentages of NAC-8/pDNA and NAC-10/pDNA polyplexes were 72% and 70%, respectively.

3.10. In vitro transfection

The transfection efficiency of polyplexes was studied in HEK 293 cells in the absence and presence of 10% FBS. To determine the transfection efficiency at cellular level, we performed FACS analysis of GFP transfected cells. The NAC-6/pGFP polyplexes exhibited about 10-fold (81.5% GFP positive cells in absence of FBS and 80.5% GFP positive cells in the presence of 10% FBS) higher transfection efficiency in comparison to chitosan/pGFP polyplexes (Fig. 7A). The results of the quantitative assessments were well accorded with the confocal microscope observation as depicted in Fig. 7B.

The transfection efficiency at protein level was evaluated by quantifying β-galactosidase activity. The amount of β-galactosidase activity was expressed in terms of milliunit of β-galactosidase/mg of the total protein. As shown in Fig. 7C, NAC polymers induced a 15–25-fold elevation in the transfection efficiency as compared to chitosan in the absence and presence of

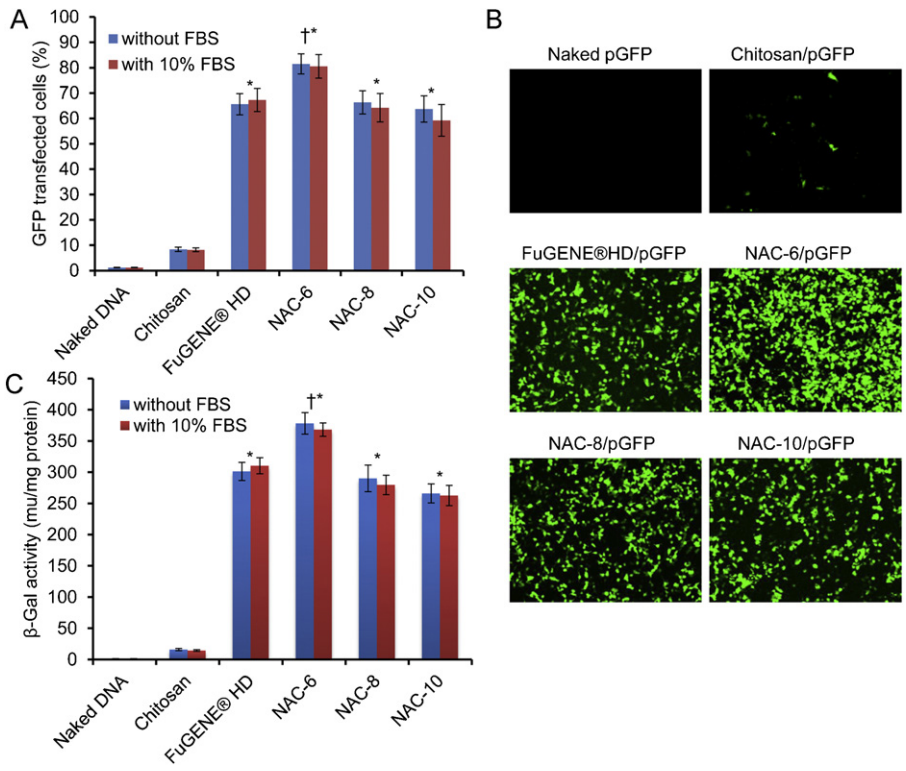

Fig. 7. In vitro transfection efficiency of chitosan and NAC polyplexes in HEK 293 cells at N/P ratio of 5 and 20, respectively. (A) Transfection efficiency at cellular level using green fluorescence protein encoding plasmid DNA (pGFP). (B) Confocal images of pGFP transfected HEK 293 cells (in serum free medium). Images were taken at 10× magnification after 48 h of transfection. (C) Transfection efficiency at protein level using beta galactosidase encoding plasmid DNA (pβ-Gal). For (A) and (C) data were expressed as mean ± S.D. ($n = 4$). ['*' indicates significant ($p < 0.001$) different from chitosan and '†' indicates significant ($p < 0.001$) different from FuGENE® HD].

10% FBS. The transfection efficiency of the polymer increased with decreasing chain length of fatty acids and NAC-6/pβ-Gal polyplex showed maximum transfection. The NAC-6/pβ-Gal polyplex induced a significantly ($p < 0.001$) higher transfection in comparison to NAC-8/pβ-Gal and NAC-10/pβ-Gal polyplexes.

In order to compare the transfection efficiency of the polymers with other non-viral gene vectors, FuGENE® HD was used as a positive control. NAC-6 polyplexes showed significantly ($p < 0.001$) higher transfection efficiency as compared to FuGENE® HD, in the absence and presence of 10%FBS. The increased transfection efficiency of NAC polymers when compared to chitosan might be explained through the collective effect of improved water solubility at neutral pH, increased uptake of the polyplexes through endocytosis, and increased release profile of pDNA from polymers. The superior transfection efficiency of NAC-6 polyplexes over other polyplexes might be attributed to the smaller size of the polyplexes and proper balance between hydrophilic–hydrophobic moieties in this polymer, thereby improving the cellular uptake of these polyplexes.

4. Conclusions

A series of N-acyl chitosan polymers were synthesized to obtain an optimum chain length of fatty acid for gene delivery application. The NAC/pDNA polyplexes exhibited suitable physicochemical properties, particle size, zeta potential, and morphology for nucleic acid delivery. The NAC polymers exhibited excellent pDNA binding ability and efficiently protected the pDNA from DNase-I degradation. Polyplexes prepared with NAC polymers exerted a rapid in vitro release of condensed pDNA compared to chitosan polyplex. The polymers as well as polymer/pDNA polyplexes did not significantly ($p > 0.05$) alter the cell viability, demonstrating a prerequisite characteristic for any successful gene delivery vector. It was found that cell uptake and transfection efficiency of chitosan was increased by several fold after modification with short chain fatty acyl moiety and increased with a decrease of acyl chain length of NAC. Among the different polymeric vectors, NAC-6/pDNA polyplexes demonstrated significantly higher ($p < 0.001$) transfection efficiency in comparison to standard commercial non-viral transfecting agent FuGENE® HD. Our results suggest that these novel NAC polymers hold a promising future in the area of gene delivery and can be used for both in vitro and in vivo applications.

Acknowledgement

This work was financially supported by the grant from the Fraternal Order of Eagles.

Appendix A. Supplementary data

Supplementary data associated with this article can be found, in the online version, at doi:10.1016/j.carbpol.2012.03.021.

References

Benns, J. M., Mahato, R. I., & Kim, S. W. (2002). Optimization of factors influencing the transfection efficiency of folate-PEG-folate-graft-polyethylenimine. *Journal of Controlled Release*, *79*, 255–269.

Chang, K. L., Higuchi, Y., Kawakami, S., Yamashita, F., & Hashida, M. (2010). Efficient gene transfection by histidine-modified chitosan through enhancement of endosomal escape. *Bioconjugate Chemistry*, *21*, 1087–1095.

Chen, X., Ding, S., Qu, G., & Zhang, C. (2008). Synthesis of novel chitosan derivatives for micellar solubilization of cyclosporine A. *Journal of Bioactive and Compatible Polymers*, *23*, 563–578.

Chen, H. H., Ho, Y. P., Jiang, X., Mao, H. Q., Wang, T. H., & Leong, K. W. (2008). Quantitative comparison of intracellular unpacking kinetics of polyplexes by a model constructed from quantum Dot-FRET. *Molecular Therapy*, *16*, 324–332.

Choksakulnimitr, S., Masuda, S., Tokuda, H., Takakura, Y., & Hashida, M. (1995). In vitro cytotoxicity of macromolecules in different cell culture systems. *Journal of Controlled Release, 34*, 233–241.

Fischer, D., Li, Y. X., Ahlemeyer, B., Krieglstein, J., & Kissel, T. (2003). In vitro cytotoxicity testing of polycations: Influence of polymer structure on cell viability and hemolysis. *Biomaterials*, *24*, 1121–1131.

Germershaus, O., Mao, S. R., Sitterberg, J., Bakowsky, U., & Kissel, T. (2008). Gene delivery using chitosan trimethyl chitosan or polyethylene glycolgraft-trimethyl chitosan block copolymers: Establishment of structure-activity relationships in vitro. *Journal of Controlled Release*, *125*, 145–154.

Godbey, W. T., Wu, K. K., & Mikos, A. G. (1999). Poly(ethylenimine) and its role in gene delivery. *Journal of Controlled Release*, *60*, 149–160.

Hirano, S., Kaneko, H., & Kitagawa, M. (1991). N-lower-fatty-acyl derivatives of chitosan as adsorbents for lysozyme and chitinase. *Agricultural and Biological Chemistry*, *55*, 1683–1684.

Hu, F. Q., Zhao, M. D., Yuan, H., You, J., Du, Y. Z., & Zeng, S. (2006). A novel chitosan oligosaccharide-stearic acid micelles for gene delivery: Properties and in vitro transfection studies. *International Journal of Pharmaceutics*, *315*, 158–166.

Huang, M., Fong, C. W., Khorc, E., & Lim, L. Y. (2005). Transfection efficiency of chitosan vectors: Effect of polymer molecular weight and degree of deacetylation. *Journal of Controlled Release*, *106*, 391–406.

Jayakumar, R., Chennazhi, K. P., Muzzarelli, R. A. A., Tamura, H., Nair, S. V., & Selvamurugan, N. (2010). Chitosan conjugated DNA nanoparticles in gene therapy. *Carbohydrate Polymers*, *79*, 1–8.

Katayose, S., & Kataoka, K. (1998). Remarkable increase in nuclease resistance of plasmid DNA through supramolecular assembly with poly(ethylene glycol)-poly(l-lysine) block copolymer. *Journal of Pharmaceutical Sciences*, *87*, 160–163.

Kawabata, K., Takakura, Y., & Hashida, M. (1995). The fate of plasmid DNA after intravenous injection in mice: Involvement of scavenger receptors in its hepatic uptake. *Pharmaceutical Research*, *12*, 825–830.

Kim, T. H., Jiang, H. L., Jere, D., Park, I. K., Cho, M. H., Nah, J. W., et al. (2007). Chemical modification of chitosan as a gene carrier in vitro and in vivo. *Progress in Polymer Science*, *32*, 726–753.

Koping-Hoggard, M., Tubulekas, I., Guan, H., Edwards, K., Nilsson, M., & Varum, K. M. (2001). Chitosan as a nonviral gene delivery system structure–property relationships and characteristics compared with polyethylenimine in vitro and after lung administration in vivo. *Gene Therapy*, *8*, 1108–1121.

Koping-Hoggard, M., Varum, K. M., Issa, M., Danielsen, S., Christensen, B. E., Stokke, B. T., et al. (2004). Improved chitosan-mediated gene delivery based on easily dissociated chitosan polyplexes of highly defined chitosan oligomers. *Gene Therapy*, *11*, 1441–1452.

Lee, K. Y., Kwon, I. C., Kim, Y. H., Jo, W. H., & Jeong, S. Y. (1998). Preparation of chitosan self-aggregates as a gene delivery system. *Journal of Controlled Release*, *51*, 213–220.

Li, Z. T., Guo, J., Zhang, J. S., Zhao, Y. P., Lv, L., Ding, C., et al. (2010). Chitosangraft-polyethylenimine with improved properties as a potential gene vector. *Carbohydrate Polymers*, *80*, 254–259.

Liu, W. G., Zhang, X., Sun, S. J., Sun, G. J., Yao, K. D., Liang, D. C., et al. (2003). N-Alkylated chitosan as a potential nonviral vector for gene transfection. *Bioconjugate Chemistry*, *14*, 782–789.

Lu, B., Wang, C. F., Wu, D. Q., Li, C., Zhang, X. Z., & Zhuo, R. X. (2009). Chitosan based oligoamine polymers: Synthesis, characterization, and gene delivery. *Journal of Controlled Release*, *137*, 54–62.

Mao, S., Shuai, X., Unger, F., Simon, M., Bi, D., & Kissel, T. (2004). The depolymerization of chitosan: Effects on physicochemical and biological properties. *International Journal of Pharmaceutics*, *281*, 45–54.

Muzzarelli, R. A. A. (1983). Chitosan and its derivatives: New trends of applied research. *Carbohydrate Polymers*, *3*, 53–75.

Muzzarelli, R. A. A., Frega, N., Miliani, M., Muzzarelli, C., & Cartolari, M. (2000). Interactions of chitin, chitosan N-lauryl chitosan and N-dimethylaminopropyl chitosan with olive oil. *Carbohydrate Polymers*, *43*, 263–268.

Park, I. K., Park, Y. H., Shin, B. A., Choi, E. S., Kim, Y. R., Akaike, T., et al. (2000). Galactosylated chitosan-graft-dextran as hepatocyte-targeting DNA carrier. *Journal of Controlled Release*, *69*, 97–108.

Piest, M., & Engbersen, J. F. J. (2010). Effects of charge density and hydrophobicity of poly(amido amine)s for non-viral gene delivery. *Journal of Controlled Release*, *148*, 83–90.

Pillai, C. K. S., Paul, W., & Sharma, C. P. (2009). Chitin and chitosan polymers: Chemistry solubility and fiber formation. *Progress in Polymer Science*, *34*, 641–678.

Sajomsang, W., Ruktanonchai, U., Gonil, P., Mayen, V., & Opanasopit, P. (2009). Methylated *N*-aryl chitosan derivative/DNA complex nanoparticles for gene delivery: Synthesis and structure–activity relationships. *Carbohydrate Polymers*, *78*, 743–752.

Thanou, M., Florea, B. I., Geldof, M., Junginger, H. E., & Borchard, G. (2002). Quaternized chitosan oligomers as novel gene delivery vectors in epithelial cell lines. *Biomaterials*, *23*, 153–159.

Tien, C. L., Lacroix, M., Szabo, P. I., & Mateescu, M. A. (2003). N-acylated chitosan: Hydrophobic matrices for controlled drug release. *Journal of Controlled Release*, *93*, 1–13.

Toh, E. K. W., Chen, H. Y., Lo, Y. L., Huang, S. J., & Wang, L. F. (2011). Succinated chitosan as a gene carrier for improved chitosan solubility and gene transfection. *Nanomedicine: Nanotechnology, Biology and Medicine*, *7*, 174–183.

Wang, B., He, C., Tang, C., & Yin, C. (2011). Effects of hydrophobic and hydrophilic modifications on gene delivery of amphiphilic chitosan based nanocarriers. *Biomaterials*, *32*, 4630–4638.

Wiethoff, C. M., & Middaugh, C. R. (2003). Barriers to nonviral gene delivery. *Journal of Pharmaceutical Sciences*, *92*, 203–217.

Zhu, A. P., Pan, Y. N., Liao, T. Q., Zhao, F., & Chen, T. (2008). The synthesis and characterization of polymerizable and biocompatible N-maleic acyl-chitosan. *Journal of Biomedical Materials Research Part B: Applied Biomaterials*, *85B*, 489–495.